ACADEMIA ROMÂNĂ
Revue Roumaine de Chimie
http://web.icf.ro/rrch/

Rev. Roum. Chim.,
2019, *64*(2), 153-162
Doi: 10.33224/rrch.2019.64.2.05

EQUILIBRIUM AND KINETIC STUDIES OF ANIONIC SURFACTANT REMOVAL BY ADSORPTION AND PHOTOCATALYTIC DEGRADATION USING HYDROTALCITE-LIKE COMPOUNDS AND THEIR CALCINED PRODUCTS

Farid AOUDJIT,[a,*] Ouiza CHERIFI[a,b] and Djamilla HALLICHE[b]

[a] Laboratory of Petrochemical Synthesis, Faculty of Hydrocarbons and Chemistry, University of M'Hamed Bougara, Boumerdes 35000, Algeria
[b] Laboratory of Natural Gas Chemistry, Faculty of Chemistry, University of Sciences and Technology,Houari Boumediene, BP 32 El-Allia, Bab Ezzouar, Algiers 16 111, Algeria

Received December 4, 2017

Due to the abundant use of anionic surfactants in our life and their disposal in the environment, the removal of surfactants from waste water becomes necessary.
The present study focused to the synthesis and application of layered double hydroxides and their derived oxides to remove the anionic surfactant, sodium dodecyl sulphate (SDS), from aqueous solution by adsorption and photocatalytic degradation under UV irradiation. The influencing of Zn^{2+}/Al^{3+} molar ratio and initial SDS concentration on the adsorption and photocatalytic degradation of SDS are studied and optimized. The obtained adsorption data were correlated with Langmuir and Freundlich isotherms models. Equilibrium studies indicated that the SDS removal obeyed Langmuir type of adsorption. Kinetic data were better described by pseudo-second-order model. The photocatalytic degradation of SDS has been found to fit the first-order kinetics according to the Langmuir–Hinshelwood model.

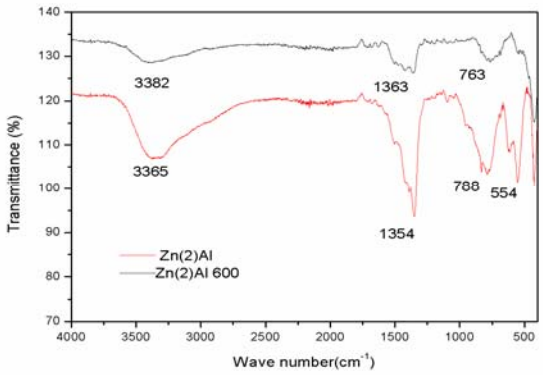

INTRODUCTION

Anionic surfactants are present in a large variety of products like soaps, detergents, and personal care products and are widely used in many industrial applications. After use, residual surfactants are discharged into sewage systems. It is reported that in domestic sewage, the anionic surfactants concentration may vary from 1 to 18 mg/L and in industrial waste water the concentration reaches up to 300 mg/L.[1,2] Many environmental and public health regulatory authorities have fixed stringent limits for the anionic surfactants standard of 0.5 mg/L for drinking water and 1.0 mg/L for other purposes. [3]

Many processes have been proposed for the surfactants removal, such as coagulation,[4, 5] photocatalytic degradation[6, 7] and adsorption.[8, 9] Among the currently used techniques, adsorption has received considerable attention due to its high removal efficiency and low-cost. Layered double hydroxides (LDH) are receiving more and more attention in recent years because it is environment-friendly and cost-effective. Layered double hydroxides

* Corresponding author: faoudjit@yahoo.fr

(LDH), also known as hydrotalcite-like compounds, are a class of synthetic anionic layered clays containing brucite-like layers and positively-charged sheets. They can be represented by the general formula: $\left[M_{1-x}^{2+}M_{x}^{3+}(OH)_2\right]^{x+}.(A_{x/n}^{n-}).mH_2O$; where M^{2+} and M^{3+} are the divalent and trivalent cations, respectively, A^{n-} represents the interlayer anion with a charge *(n-)* and *x* is equal to the ratio of $M^{3+}/(M^{2+} + M^{3+})$ with a value varying in the range of 0.17–0.50. LDH materials present properties like layered structure, high porosity, high surface area, and interlayer anion mobility.

The purpose of this study is to investigate the adsorption and photocatalytic degradation under UV irradiation of SDS surfactant on the uncalcined and calcined LDH materials, synthesized with different cationic ratios (Zn/Al). Many parameters such Zn^{2+}/Al^{3+} molar ratio, initial SDS concentration are investigated. Isotherms and kinetics analysis are detailed in this study.

EXPERIMENTAL

Materials preparation

All chemicals were analytical grade and used as received without further purification.

The materials types LDH were prepared by the co-precipitation method at constant pH (11) with cationic ratio (Zn^{2+}/Al^{3+}) of 2, 3 and 4. In this method, 100 mL of solution containing a fixed amount of $Zn(NO_3)_2{\cdot}6H_2O$ (0.14 moles) and $Al(NO_3)_3{\cdot}9H_2O$ (0.066, 0.045 and 0.034 moles) were added dropwise, to 100 mL of an alkaline solution containing NaOH (0.3 moles) and Na_2CO_3 (0.094 moles) under vigorous stirring. The resulting slurry was hydrothermally treated; it was placed for 8 h on oil bath at 60 °C under magnetic stirring and reflux. The final products were recuperated by filtration, washed several times with distilled water until reaching pH ≈ 7 and the precipitates obtained were dried at 80 °C overnight.

The calcined LDH was obtained by calcination of LDH samples in a muffle furnace at 600 °C for 4 h, with heating in increments of 5 °C /min.

The dried samples were denoted as Zn(r)Al and calcined samples denoted as Zn(r)Al600, where *r* stands for the cationic ratio (2, 3 and 4) and 600 is the calcination temperature.

Materials characterization

The crystalline phases of samples were identified by X-ray powder diffraction (XRD) using Panalytical X'Pert PRO MPD diffractometer with filtered Cu Kα radiation in 2θ range from 5 to 70°. The texture of samples was analysed by low temperature nitrogen adsorption at -196 °C (Micromiritics ASAP 2000) using Quantachrome Autosorb 1-MPautomated gas adsorption system. Fourier transform infrared (FTIR) spectra were recorded on a Bruker ALPHA spectrophotometer, at a resolution of 2 cm^{-1} and averaging over 20 scans, in the range 400 cm^{-1} – 4000 cm^{-1}. The morphology of the samples was investigated using scanning electron microscopy (Quanta 250) with an accelerating voltage of 20 kV, combined with energy dispersive X-ray spectroscopy (Système EDX Bruker EDS Quantax 200) for the determination of materials composition.

Adsorption studies

The adsorption study was carried out using the batch method. It was performed by introducing a given amount of adsorbent into 100 mL Erlenmeyer flasks containing 50 mL of an aqueous SDS solution with desired concentration. The mixture was shaken for the desired period at 25°C using a shaking rotating incubator (KS 4000, IKA, Germany) at 200 rpm. After shaking period, the mixture was then filtered, and the filtrate was analyzed by UV–vis spectrophotometer at 648 nm to determine the residual concentration of SDS using a simplified spectrophotometric method developed by Jurado.[10] Adsorption experiments were conducted by varying, adsorbent dose, initial SDS concentration, contact time and temperature.

The adsorption capacity q_t *(mg/g)* is calculated using the following equation:

$$q_t = \frac{(C_0 - C_t)}{m} \times V$$

where C_0 and C_t are the initial concentration and concentration at time *(t)* of SDS, *V* is the volume of SDS solution *(L)* and *(m)* is the mass of adsorbent *(g)*.

Photocatalytic degradation studies

The photocatalytic degradation experiments were carried out using a 500 mL double-glass cylindrical reactor. The temperature in this reactor is controlled by the constant circulation of water. The SDS solution with photocatalyst were magnetically stirred using a magnetic stirrer. The radiation source used was a 100 watt UV lamp (type Black-Ray B100AP UV 230 V-50 Hz), with maximum emission at 365 nm. The desired dose of photocatalyst was introduced into the reactor vessel containing 100 mL of SDS solution with desired concentration. Prior to irradiation, the solution was magnetically stirred in the dark for 60 min to allow the adsorption of SDS to the photocatalyst. 5 mL of the solution was withdrawn from the reactor vessel periodically and filtered. Then the filtrate was analyzed by UV–vis spectrophotometry at 648 nm to determine the residual concentration of SDS.

The SDS removal efficiency was calculated as follows:

$$R(\%) = \frac{(C_0 - C_t)}{C_0} \times 100$$

where C_0 and C_t are the initial concentration and concentration at time *(t)* of SDS.

RESULTS AND DISCUSSION

Characterization

X-ray diffraction (XRD)

The XRD patterns of Zn(2)Al and Zn(2)Al600 are shown in Fig. 1. It could be seen clearly from this figure that the XRD patterns of Zn(2)Al exhibit a

series of characteristic reflections of well-crystallized hydrotalcite-like structure, which are sharp and symmetric at low *2θ* angle (planes of 003, 006 and 012), but broad and asymmetric at high *2θ* angle (planes of 015, 018 and 110).[11, 12] As seen from the XRD patterns of Zn(2)Al600 (calcined sample at 600 ◦C), the (003) and (006) reflections observed in the Zn(2)Al practically disappeared indicating that the hydrotalcite structure is destroyed and there is disordering in the stacking of the layers and only ZnO peaks are observed.

Lattice parameters of the Zn(2)Al sample (d_{003}, d_{110}, *c* and *a*) are shown in Table 1.

The cell parameters were calculated as $a = 2 \times d_{110}$ and $c = 3 \times d_{003}$, respectively. [13]

The unit cell parameter *(a)* is the average distance between two metal ions in the brucite-like layers and *(c)* is three times the distance from the center of one layer to the next, and is directly related to the layer charge density and size as well as to the interlayer anionic electrostatic interaction.

Fourier transform infrared spectroscopy analysis (FTIR)

The Fig. 2 shows the FTIR spectra of Zn(2)Al and Zn(2)Al600 samples. A strong broad absorbance band appears at around 3365 cm^{-1}, which is attributed to the hydroxyl group stretching vibration in the brucite-like layers and the interlayer water molecules.[14, 15] The band observed at about 1354 cm^{-1} is assigned to the asymmetric stretching mode of the carbonate anions.[16, 17] Finally, the bands ranging from 400 to 800 cm^{-1} can be attributed to the characteristic stretching bands of M-O and O-M-O vibration.[18-20] As seen from the FTIR spectrum of the calcined sample Zn(2)Al600 all the absorption bands are weakened, compared to the as synthesized Zn(2)Al, the peak intensity of CO_3^{2-} ions at 1363 cm^{-1} become relatively weaker, indicating that more CO_3^{2-} ions in the interlayer are removed.

Brunauer-Emmer-Teller analysis (BET)

The structure parameters of the studied samples such as the BET surface area, average pore-size and pore volume are listed in Table 2.

The samples exhibit a strong characteristic of mesoporous materials[21,22] and this result is further confirmed by the well-developed mesopores with diameters of 6.475 and 4.571 nm (2< d <50 nm) given in Table 2.

Table 1

Cell parameters and crystallite sizes of Zn(2)Al

Adsorbent	Unit cell parameter (nm)		Crystal size (nm)	
	c	a	d_{003}	d_{110}
Zn(2)Al	2.3064	0.3081	0.7688	0.1540

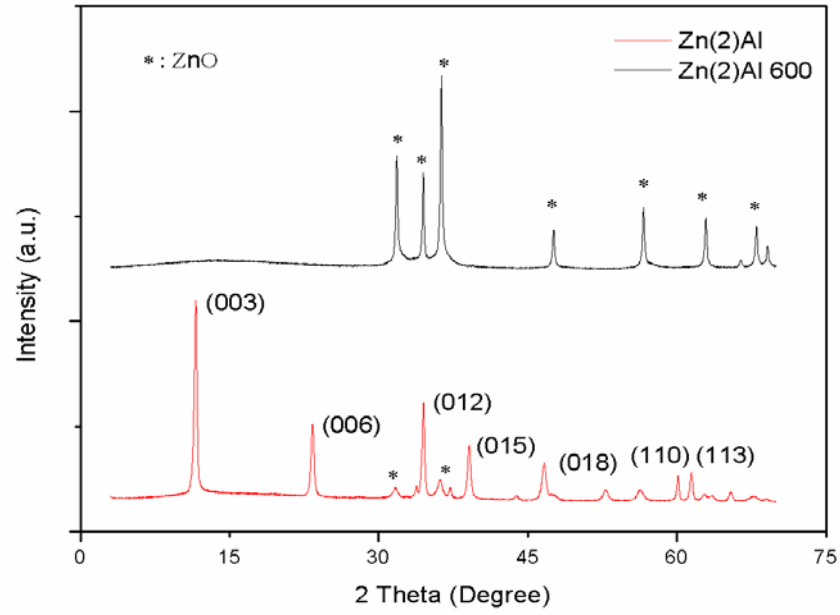

Fig. 1 – XRD patterns of Zn(2)Al and Zn(2)Al600.

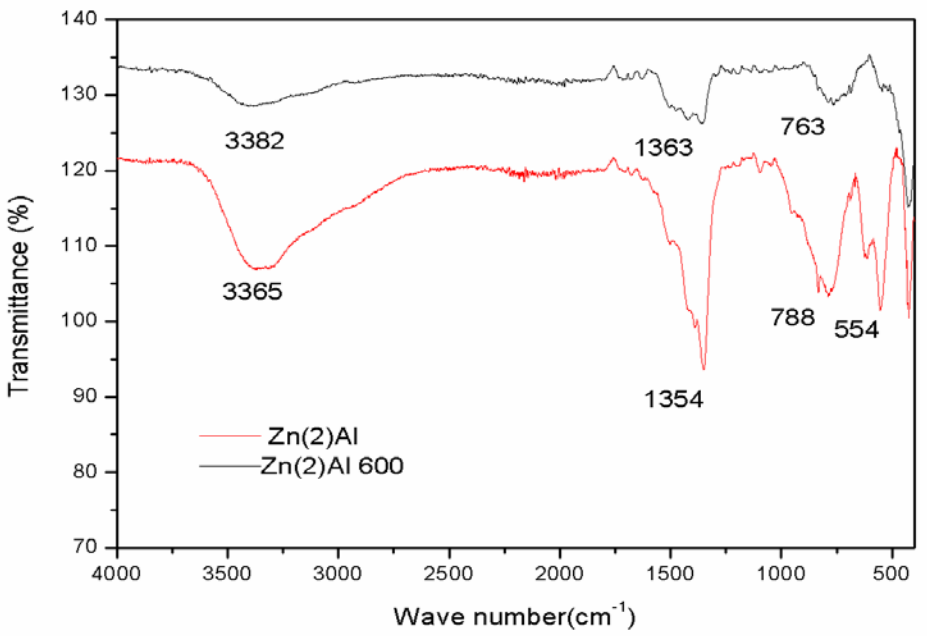

Fig. 2 – FTIR spectra of Zn(2)Al and Zn(2)Al600.

Table 2

Summary of BET analysis results of Zn(2)Al and Zn(2)Al600

Adsorbent	BET surface area (m^2/g)	Pore volume (cm^3/g)	Average pore diameter (nm)
Zn(2)Al	33.21	0.0537	6.4754
Zn(2)Al600	72.08	0.0823	4.571

The BET surface area of the calcined sample (Zn(2)Al600) is 72.08 m^2/g which is higher than that of the uncalcined sample (33.21 m^2/g).The pore volume values of the calcined LDH are also increasing. When the synthesized solids are calcined, the lamellar structure collapses, which produced cavities or crates resulting in larger surface areas.

Energy dispersive X-ray spectroscopy

The final composition of the synthesized samples was determined by high energy dispersive X-ray spectrometer. The results obtained are presented in Table 3.

The x (M^{3+}/M^{2+} + M^{3+}) value obtained for Zn(2)Al was 0.35 the obtained value is between 0.2 and 0.35, which is considered as the optimum value for the preparation of pure LDH structures.[13]

Adsorption studies

Effect of Zn/Al molar ratio and calcination on SDS adsorption

The effect of varying Zn/Al molar ratio of LDH on the SDS removal was investigated with three different ratios of 2, 3 and 4. Fig. 3 shows that the removal capacity decreased with increasing Zn/Al molar ratio. This could be due to the fact that Zn(2)Al contains a higher amount of Al^{3+} and the net positive charge on the hydroxide layer was higher than Zn(3)Al and Zn(4)Al.

Table 3

Chemical formula and chemical composition Samples based on the EDX results

Adsorbent	Zn (wt%)	Al (wt%)	Zn (Atom%)	Al (Atom%)	Zn^{2+}/Al^{3+} molar ratio	X	Chemical formula
Zn(2)Al	54.17	13.86	24.45	15.15	1.61	0.35	$Zn_{0.65}Al_{0.35}$
Zn(2)Al 600	61.56	11.60	30.88	14.09	-	-	-

$x = Al^{3+}/(Zn^{2+} + Al^{3+})$

Fig. 3 also shows that adsorption of SDS on calcined LDH was appreciably higher than the LDH. The increase in adsorption capacity of calcined LDH may be due to two main reasons: (i) the increase of specific surface area by calcination treatment and simultaneously the release of intercalated anions (mainly CO_3^{2-}) from the precursor interlayer space, which produces more active sites for SDS adsorption; and (ii) the increase of positive surface charge by calcination treatment, which contributes to an electric charge effect between the oxides and SDS molecules which are negatively charged in aqueous solution.[23, 24]

Effect of contact time and initial SDS concentration

The Fig. 4 shows that the equilibrium adsorption increases with increasing contact time at all initial SDS concentrations and equilibrium adsorption state was reached after 120 min. This short equilibrium time often reflects the physical adsorption.[25]

The adsorption capacity of SDS increases with increasing initial SDS concentration. The increase in adsorption capacity with increasing initial concentration of SDS can be explained by the existence of a higher concentration gradient, which increases the diffuse contribution of the mass transfer process. The higher concentration of adsorbate in the solution increases the electrostatic repulsion between molecules in the medium, increasing the diffuse resistance to mass transfer within the solution.

Kinetic studies

Pseudo first- order and pseudo-second-order kinetic models were applied to the data at different initial concentrations of SDS. The results of the kinetics parameters of SDS adsorption on Zn(2)Al and Zn(2)Al600 are presented in Table 4.

According to the Tab. 4 the R^2 values of the pseudo-second order were observed to be close to 1 with all initial concentrations which were higher than those of pseudo-first-order.

Moreover, calculated, q_e *cal* values from pseudo-second-order fitting model are very close to the experimental q_e values (Table 4). From these observations, it can be concluded that the pseudo-second-order kinetic model is more applicable for describing the adsorption process of SDS on the prepared Zn(2)Al and Zn(2)Al600. It is suggested that the SDS adsorption was controlled by chemisorption involving the valence forces through sharing or exchange of electrons between adsorbent and adsorbate.

Adsorption Isotherms

In the present study the Langmuir and Freundlich isotherms have been chosen to explain the sorption mechanisms and the surface properties of the adsorbents.

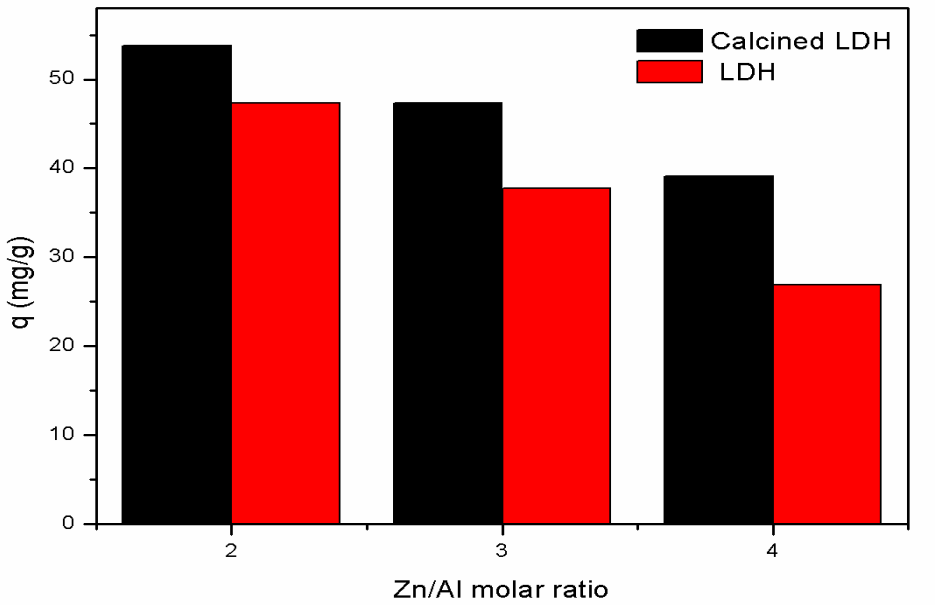

Fig. 3 – Effect of (Zn/Al) molar ratio and calcination on SDS adsorption (C_0 =100 mg/L, adsorbent dose= 1g/L, pH = neutral, T= 25°C, contact time = 160 min, stirring speed= 200 rpm).

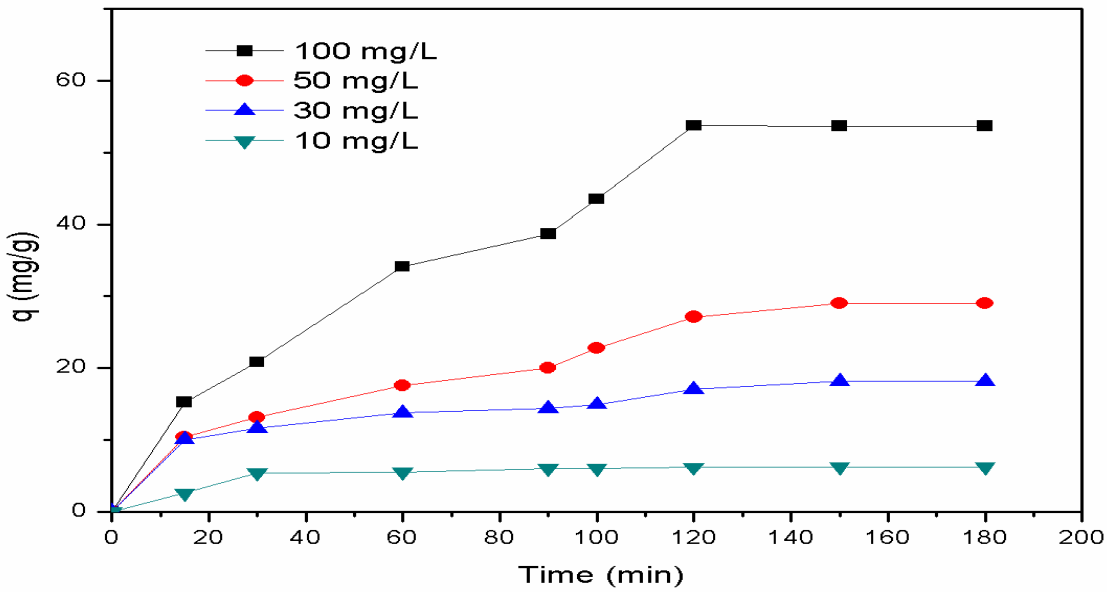

Fig. 4 – Effect of contact time and initial concentration on SDS removal by Zn(2)Al600 (adsorbent dose= 1g/L, pH = neutral, T= 25°C, stirring speed= 200 rpm).

Table 4

Parameters for the adsorption of SDS on Zn(2)Al and Zn(2)Al 600 at different initial concentrations

Adsorbent Initial concentration (mg/L)	Pseudo first order constant			Pseudo second order constant				$q_{e,exp}$ (mg/g)
	$K_1 . 10^{-2}$ (min^{-1})	$q_{e,cal}$ (mg/g)	R^2	$K_2 . 10^{-4}$ (g/mg. min)	$q_{e,cal}$ (mg/g)	h (mg/g.min)	R^2	
Zn(2)Al								
100	3.082	72.515	0.6304	0.918	106.382	1.039	0.9953	43.675
50	1.953	27.267	0.9123	8.836	33.411	0.986	0.9938	24.302
30	1.581	13.689	0.9207	30.477	14.170	0.611	0.9951	15.49
10	1.979	6.689	0.7691	41.163	4.761	0.093	0.9953	5.89
Zn(2)Al 600								
100	1.519	51.289	0.9757	1.871	76.511	0.842	0.9756	53.73
50	1.313	25.324	0.9458	4.76	37.907	1.211	0.9627	29
30	1.433	12.449	0.8250	19.499	20.296	0.322	0.9767	18.169
10	2.8	5.865	0.8644	216.351	6.464	0.648	0.9991	6.2

Table 5

Isotherm parameters for SDS adsorption onto Zn(2)Al and Zn(2)Al600

Adsorbent	*Freundlich model*			*Langmuir model*				Tempkin model		
	K_f (mg/g)	n	R^2	K_l (L/ mg)	q_m (mg/g)	R^2	R_L	B (j/mol)	K_t (L/g)	R^2
Zn(2)Al	0.8968	0.9989	0.9087	0.0118	105.485	0.997	0.4585	13.580	0.313	0.9497
Zn(2)Al600	2.4743	1.257	0.9397	0.0213	90.252	0.9968	0.3189	0.318	0.526	0.9044

The linear plots of the two equilibrium models were showed in Figs. 5 and 6. The fitted constants for the two models along with regression coefficients (R^2) are summarized in Table 5.

The adsorption equilibrium data fit both Freundlich and Langmuir equations with a correlation coefficient value greater than 0.99 for both adsorbents. In our investigation for the two adsorbents, R_L was found to be between 0 and 1 indicating a favorable Langmuir adsorption.

Photocatalytic degradation studies

Effect of initial SDS concentration

In this study we varied the initial concentration of SDS in the range of 10 mg/L– 100 mg/L and the

other parameters were fixed (adsorbent dose 10 g/L, pH neutral and temperature = 25°C). As seen from Fig. 7 the photodegradation efficiency depend inversely on the initial SDS concentration. With initial SDS concentration of 10 mg/L the photodegradation efficiency was higher. This phenomenon is due to the fact that when the initial SDS concentration increase the formation rate of OH• radical decrease, which can be explained by the fact that when there are enough SDS molecules the light will be adsorbed by these molecules and the photons never reach the photocatalyst surface.[26, 27]

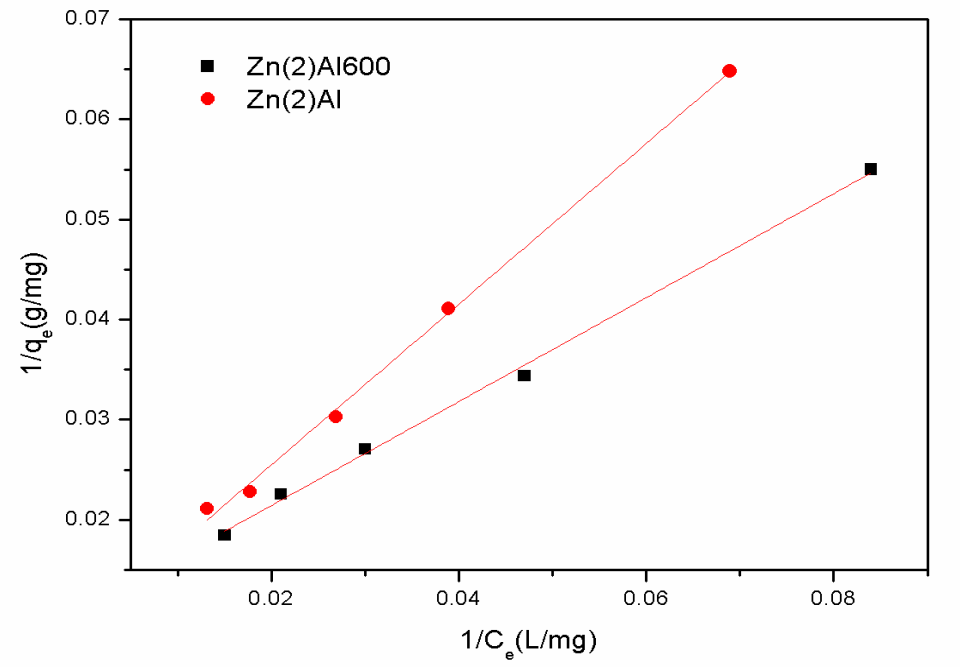

Fig. 5 – Langmuir plots for SDS adsorption on Zn(2)Al and Zn(2)Al600
(C_0 =5 - 120 mg/L, adsorbent dose= 1g/L, pH = neutral, T= 25°C, contact time = 160 min, stirring speed= 200 rpm).

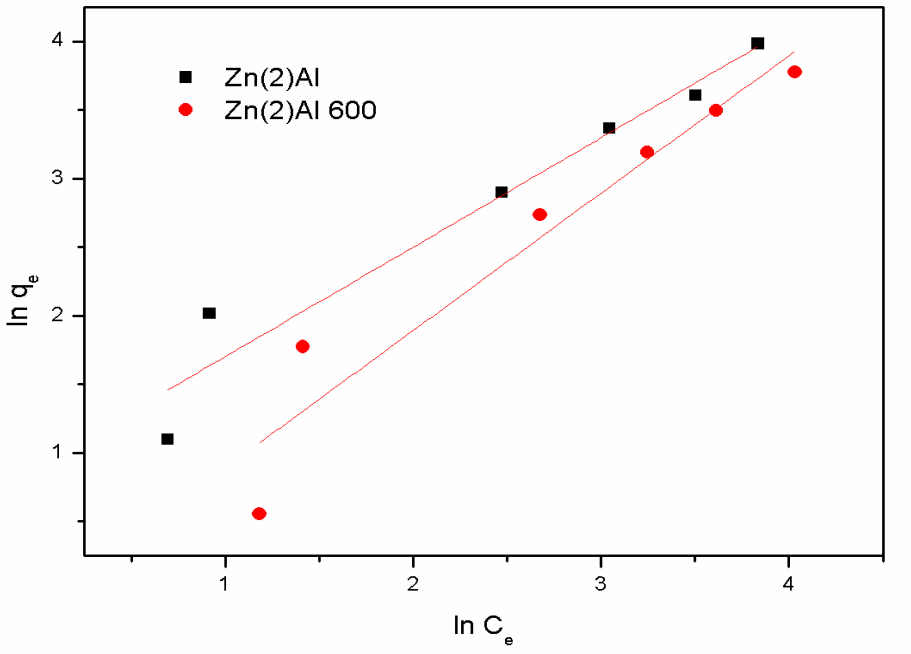

Fig. 6 – Freundlich plots for SDS adsorption on Zn(2)Al and Zn(2)Al600
(C_0 =5 - 120 mg/L, adsorbent dose= 1g/L, pH = neutral, T= 25°C, contact time= 160 min, stirring speed= 200 rpm).

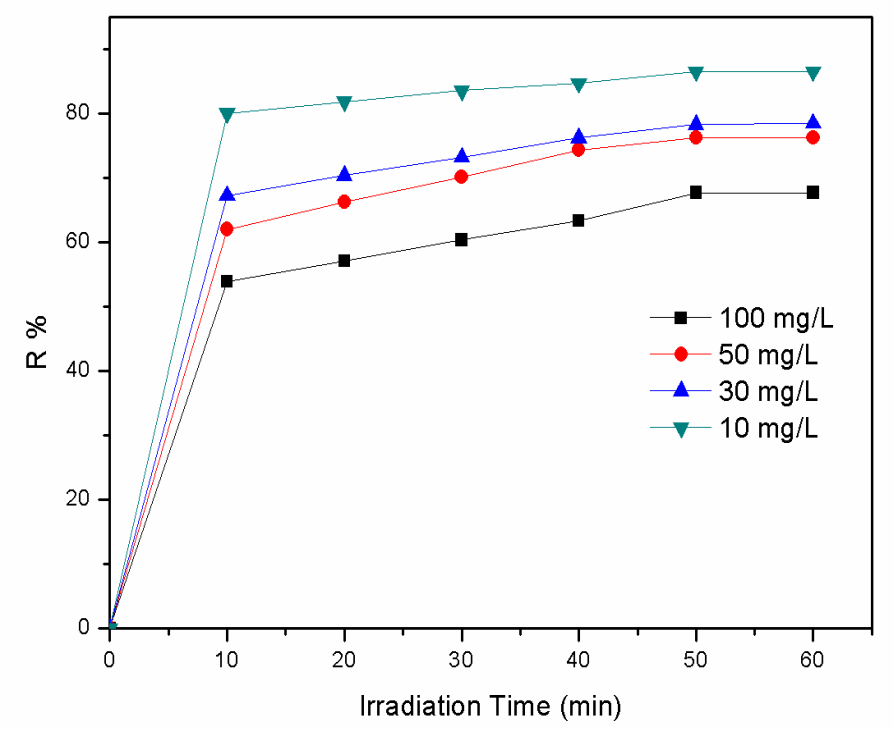

Fig. 7 – Effect of initial SDS concentration on the photodegradation of SDS by Zn(2)Al 600 (photocatalyst dose= 10 g/L, pH = neutral, T= 25 °C).

Kinetics of SDS photodegradation

The Langmuir–Hinshelwood model is commonly used to describe the kinetics of photocatalytic reactions of organic compounds in aqueous solutions. It relates the degradation rate r and the concentration of organic compound C, and is expressed as follows.

$$r = -\frac{dc}{dt} = \frac{K_r K_{ad} C}{1 + K_{ad} C}$$

where k_r is the rate constant and K_{ad} is the adsorption equilibrium constant. When the adsorption is relatively weak and the reactant concentration is low, the equation can be simplified to the first-order kinetics with an apparent rate constant K_{app}. $\ln \frac{C_0}{C} = K_{app} t$

where C_0 is the initial concentration after achieving adsorption-desorption equilibrium. Plotting $ln\ (C_0/C)$ versus irradiation time (t) yields a straight line, and the slope is the apparent rate constant $Kapp$. The half-life of the degraded organic compound can be calculated by the following equation:

$$t_{1/2} = \frac{0.693}{K_{app}}$$

Fig. 8 presents results of the SDS photodegradation kinetic studies for Zn(2)Al and Zn(2)Al 600 samples, apparent constant K_{app}, SDS half-life, and the linearization coefficient R^2 are summarized in Table 7. As shown in Table 6, the SDS photodegradation results adjusted well to the pseudo-first-order kinetic model.

Table 6

The Langmuir–Hinshelwood model parameters of photocatalytic degradation

SDS Initial concentration (mg/L)	Zn(2)Al			Zn(2)Al 600		
	K_{app} (10^{-2}) (min^{-1})	$t_{1/2}$ (min)	R^2	K_{app} (10^{-2}) (min^{-1})	$t_{1/2}$ (min)	R^2
100	0.65	106.615	0.9846	0.651	106.451	0.9812
50	0.701	98.858	0.9629	0.975	71.076	0.986
30	0.831	83.393	0.9949	1.192	58.137	0.9795
10	0.774	89.534	0.9695	1.093	63.403	0.9798

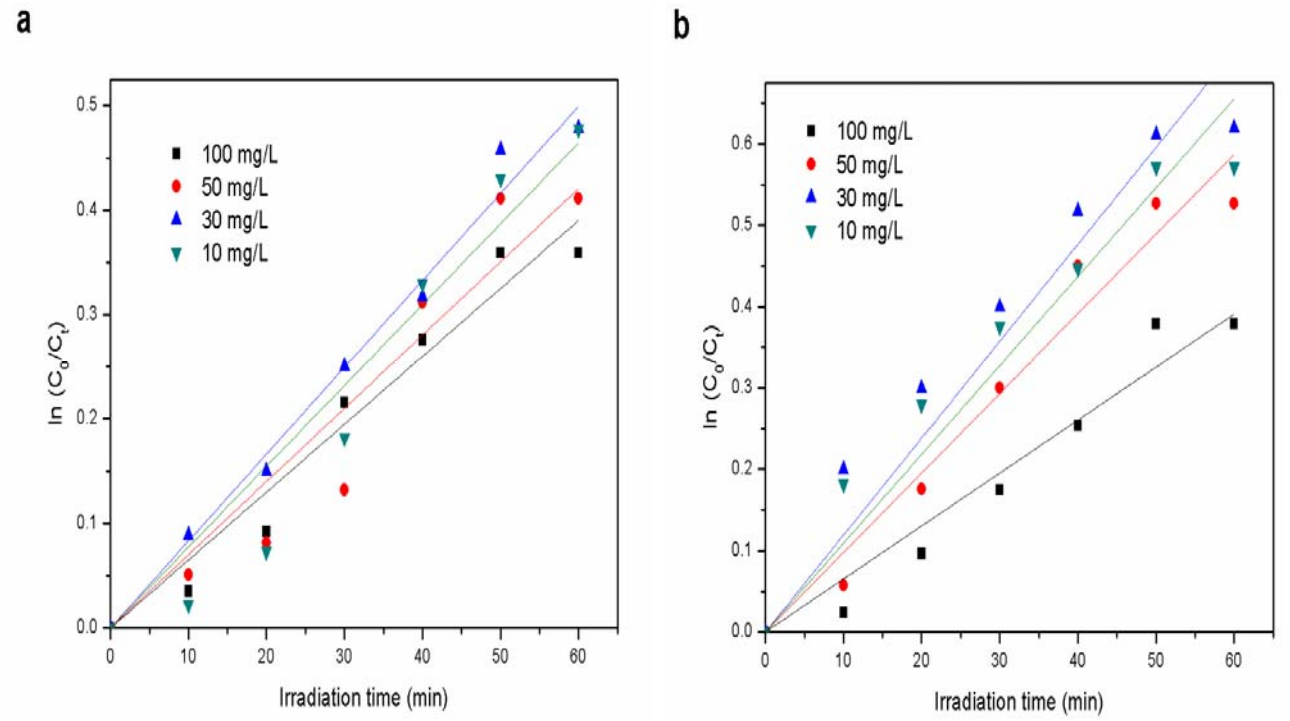

Fig. 8 – Pseudo-first-order kinetics photodegradation of SDS, by Langmuir– Hinshelwood model on Zn(2)Al and (b) Zn(2)Al 600 (photocatalyst dose= 10 g/L, pH = neutral, T= 25 ˚C).

CONCLUSION

The present study shows that both Zn(2)Al and Zn(2)Al600 prepared by coprecipitation method could be used as an effective adsorbent for the removal of SDS from aqueous solution by adsorption and photocatalyic degradation.

The $Zn^{2+/}Al^{3+}$ molar ratio and calcination were found to affect the adsorption and photodegradation process. Zn(2)Al600 with Zn/Al molar ratio of 2, calcined at a temperature of 600 ºC was found to be more efficient for SDS removal than that uncalcined Zn(2)Al. The adsorption process was found to depend on the amount of adsorbent, the initial concentration of the SDS, the contact time and the temperature.

Kinetics of SDS adsorption from aqueous solution followed a pseudo-second-order model. Adsorption isotherms indicated that SDS removal by both Zn(2)Al and Zn(2)Al600 were an endothermic process and fitted the Langmiur model well. The photocatalytic degradation of follows the first-order kinetics according to the Langmuir–Hinshelwood model.

REFERENCES

1. E. L. Terechova, G. Zhang, J. Chen, N. A. Sosnina and F. Yang, *J. Environ. Chem. Eng.*, **2014**, *2*, 2111-2119.
2. A. K. Mungray and P. Kumar, *Process Saf. Environ. Prot.*, **2009**, *87*, 254– 260.
3. E. Olkowska, M. Ruman and Ż. Polkowska, *J. Anal. Methods Chem.*, **2014**, *2*, 769-708.
4. G. A. Ciorba, C. Radovan, I. Vlaicu and L. Pitulice, *Electrochim. Acta*, **2000**, *46*, 297–303.
5. K. Ikehata and M. G. El-Din, *Ozone Sci. Eng.*, **2004**, *26*, 327–343.
6. Y. Y. Eng, V. K. Sharma and A. K. Ray, *Chemosphere*, **2010**, *79*, 205–209.
7. T. Zhang, T. Oyama, S. Horikoshi, J. Zhao, N. Serpone and H. Hikada, *Appl. Catal. B: Environ.*, **2003**, *42*, 13-20.
8. S. R. Taffarel and J. Rubio, *Miner. Eng.*, **2010**, *237*, 71–79.
9. N. Schouten, L.G. van der Ham, G.J. Euverink and A.B. de Haan, *Water Res.*, **2007**, *41*, 4233–4241.
10. E. Jurado, S. Fernandez, J. Nunez-Olea, G. Luzon and M. Lechuga, *Chemosphere*, **2006**, *65*, 278–285.
11. C. Busetto, G. Del Piero, G. Mamara, F. Trifiró and A. Vaccari, *J. Catalysis*, **1984**, *85*, 260–266.
12. F. Cavani, F. Trifiro and A. Vaccari, *Catal. Today*, **1991**, *11*, 173–301.
13. D. G. Cantrell, L. J. Gillie, A. F. Lee and K. Wilson, *Appl. Catal. A Gen.*, **2005**, *287*, 183–190.
14. X. Cheng, X. Huang, X. Wang and D. Sun, *J. Hazard. Mater.*, **2010**, *177*, 516–523.
15. J. T. Kloprogge, D. Wharton, L. Hickey and R. L. Am, *Mineral.*, **2002**, *8*, 623–629.
16. H. Toshiyuki, Y. Yasumasa, K. Katsunori and T. Atsumu, *Clays and Clay Minerals*, **1995**, *43*, 427-432.
17. B. Dudek, P. Kustrowski, A. Białas and P. Natka, *Mater. Chem. Phys.*, **2012**, *132*, 929-936.
18. W. Dongjin, L. Yongde, X. Shuhu, C. Jing and Z. Jian, *Colloids and Surfaces A: Physicochem.*, **2015**, *469*, 307–314.
19. M. Tong, H. Chen, Z. Yang and R. Wen, *Int. J. Mol. Sci.*, **2011**, *12*, 1756-1766.

20. D. Chaara, I. Pavlovic, F. Bruna, M. A. Ulibarri, K. Draoui and C. Barriga, *Appl. Clay Scie.*, **2010**, *50*, 292–298.
21. G. Wu, X. Wang, B. Chen, J. Li, N. Zhao, W. Wei and Y. Sun, *Appl. Catal. A: Gen*., **2007**, *329*, 106–111.
22. J. Zhou, S. Yang, J. Yu and Z. Shu, *J. Hazard. Mater.*, **2011**, *192*, 1114–1121.
23. C. L. Zhang, Y. Baojun, Z. Shengnan, W. Bainian and X. Bing, *J. Mater. Chem. A*, **2014**, *2*, 10202-10208.
24. Z. Tong, P. Zheng, B. Bai, H. Wang and Y. Suo, *Catalysts*, **2016**, *6*, 58-64.
25. A. Akyol, H. C. Yatmaz and M. Bayramoglu, *Appl. Catalysis B: Environ.*, **2004**, *54*, 19–24.
26. C. Changchun, L. Jiangfeng, L. Ping and Y. Benhai, *Adv. Chem. Eng. Sci.,* **2011**, *1*, 9-14.
27. O. Ozdemir, C. Mustafa, S. Eyup, A. Fatma, S. Mehmet and M. Celik, *J. Hazardous Mater.*, **2007**, *147*, 625–632.